Thermal and Physicomechanical Properties of Ethylene-vinyl Acetate Copolymer and Layered Double Hydroxide Composites

B. Ramaraj, Kuk Ro Yoon

Nano Bio-Sensor Research Team, Department of Chemistry, Hannam University, Jeonmin-dong, Yuseong-gu, Daejeon 305-811, Korea

Received 15 August 2007; accepted 6 January 2008
DOI 10.1002/app.28026
Published online 19 March 2008 in Wiley InterScience (www.interscience.wiley.com).

ABSTRACT: A series of ethylene-vinyl acetate (EVA) copolymer films have been prepared with different compositions viz. 2, 4, 6, and 8 wt % layered double hydroxide (LDH) nanoparticles by solution intercalation method. These solution-casted EVA/LDH nanocomposite films were dried and characterized by differential scanning calorimetry (DSC) and Fourier transform infrared (FTIR) spectroscopy. EVA/LDH films were further tested for tensile strength, density, moisture content, solubility resistance, flammability, and electrical properties. The DSC and FTIR analysis indicate strong interactions between the LDH layers and vinyl acetate groups in EVA. Further, EVA nanocomposite films show enhanced tensile strength, limiting oxygen index (LOI), and flammability rating for the addition of LDH without sacrificing the electrical properties. © 2008 Wiley Periodicals, Inc. J Appl Polym Sci 108: 4090–4095, 2008

Key words: ethylene-vinyl acetate copolymer; layered double hydroxides; differential scanning calorimetry; flame retardance; composites

INTRODUCTION

Ethylene-vinyl acetate copolymer (EVA) is a widely used material, particularly as a zero-halogen material in the cable industry. EVA is frequently formulated with large quantities of inorganic fillers. It is highly elastomeric and tolerates higher filler loading while retaining its flexible properties. To achieve the required flame retardant grade of low smoke and nontoxic character, metal hydroxides, mainly aluminum trihydroxide (ATH), are added in a high loading level. The higher loading level affects the processability of EVA. One possible way to reduce the necessary amount of additive is to increase its flame retardant effectiveness. Flame retardancy, in some of the earlier proposals, is improved by adding zinc borate[1] or coating with molybdenum compound[2] or zinc hydroxy stannate[3] or borosiloxane.[4] Recently, considerable improvement in flame retardancy is expected from the combined addition of modified layered silicates (nanocomposites) and traditional flame retardants such as ammonium polyphosphate[5–7] or metal hydroxide.[8,9]

Nanocomposites are particle-filled polymers for which at least one dimension of the dispersed particles is in the nanometer range. Polymer-layered silicate nanocomposites are hybrids composed of layered silicates dispersed in a polymer matrix in the form of layers of about 1-nm thick and with an aspect ratio between 100 and 1000. Lately a new emerging class of nanocomposites, based on layered double hydroxides (LDH), also known as anionic or hydrotalcite-like clays, has been investigated.[10] LDH have similar geometrical structure as the natural clay minerals such as montmorillonite (MMT), but with opposite charge of the hydroxide layers. The most remarkable aspect of LDH materials in comparison to various natural clay materials is their homogeneous composition, which allows compound designers to maintain the impurity level at minimum.

The dispersion of the nanoparticles within the polymer has significant influence on the properties of material. So, there are two critical factors to produce polymer nanocomposites, i.e. the hydrophilic nanoparticles has to be modified to make organophilic to get dispersion in organophilic polymers or nanoparticles has to be dispersed in hydrophilic polymers. Because the hydrophilicity of the nanoparticles hinders the formation of homogeneous dispersion in organic polymers.[11,12] It was found that the hydrophilic character of MMT clay promotes dispersion of these inorganic crystalline layers in hydrophilic polymers such as poly(ethylene oxide)[13] and poly(vinyl alcohol).[14,15] More recently, EVA-based nanocomposites have been developed to improve EVA's properties and further explore its applications[16–19] by melt blending process. LDH-based nanocomposites prepared by solution casting method

Correspondence to: K. R. Yoon (kryoon@hannam.ac.kr).

Journal of Applied Polymer Science, Vol. 108, 4090–4095 (2008)

showed exfoliated nature of the dispersed particles,[20–22] whereas the melt mixing method gives mostly intercalated or flocculated composites.[23] There are also reports of well dispersed nanoclay in EVA where a compatibilizing agent was not required.[24,25] This is an indication that the partial polarity of VA in EVA enhances the polymer-clay interactions. EVA/clay nanocomposites can be easily prepared because the EVA contains polar group, vinyl acetate (VA), which can effectively interact with clay. In the past, Zanetti et al.[26,27] prepared EVA/clay nanocomposites by melt blending and studied the thermal and flame retardant properties of this material. The flame retardant properties of the EVA/clay nanocomposites were also studied by Duquesne et al.[28] They conclude that a nanostructure enables to achieve better fire performance than a microstructure. Alexandre et al.[24] obtained EVA/MMT nanocomposites with a semi-intercalated and semiexfoliated structure also by melt blending and found that Young's modulus and thermal stability of the nanocomposites were enhanced. Inspired from these studies, this work is focused on investigating the properties of EVA/LDH nanocomposites by solvent casting method.

In the ongoing efforts to prepare polymeric composites,[29–31] the present study reports the preparation of EVA nanocomposite films using LDH. The primary focus of the present investigation was to explore the potential of LDH materials as filler without modification in a polar polymer like EVA by solution casting method. The properties of the EVA/LDH nanocomposite films were investigated as a function of LDH concentration.

EXPERIMENTAL

Materials

Commercial ethylene vinyl acetate copolymer (EVA) PILENE EVA 2825 containing 28% VA content and with melt flow index (190°C/2.16 kg) of 25 g/10 min supplied by M/s National Organic Chemical Industries, Mumbai, India was chosen as the matrix. Xylene (Sulfur free, boiling range 137–144°C) supplied by M/s Nice Chemicals, Cochin, India was used as solvent.

Preparation of Mg-Al layered double hydroxide

Mg-Al LDH was synthesized by urea hydrolysis method.[32,33] An aqueous solution containing Al^{3+} and Mg^{2+} with the molar fraction $Al^{3+}/(Al^{3+} + Mg^{2+})$ equal to 0.33 was prepared by dissolving $AlCl_3$ and $MgCl_2$ in distilled water. To this solution solid urea was added until the molar fraction, urea/$(Al^{3+} + Mg^{2+})$ reached 3.3. The clear solution was refluxed for 36 h. The white precipitate was then filtered, washed, and dried in vacuum at 60°C till constant weight.

Preparation of EVA/LDH nanocomposite films

Nanocomposite films were synthesized by a solvent-intercalation solution casting method: films were cast from LDH solvent suspension where EVA was dissolved in xylene. EVA solution was mixed with 2, 4, 6, and 8 wt % of LDH nanoparticles. The solid content of EVA and LDH was optimized at 4% solution in xylene and the system was made into a homogeneous solution by constant stirring at a temperature of around 110–120°C. When the homogenization was obtained, composite films were prepared by casting the solution on glass plate (35 cm × 35 cm). After drying, the films were carefully removed from the mold and used for further characterization and testing.

Characterization and testing of EVA/LDH nanocomposite films

Solution-casted nanocomposite films were analyzed by DSC (DSC 2010, TA instruments, New castle, DE) from 50 to 200°C in nitrogen atmosphere at the heating rate of 10°C/min. The maxima of melting endothermic peaks were taken as melting temperature (T_m). The melting peak area was used to calculate the enthalpy of fusion. The flammability was characterized by Underwriter Laboratory 94 test method and limiting oxygen index (LOI) measurements (ASTM D 2863). Fourier transform infrared (FTIR)

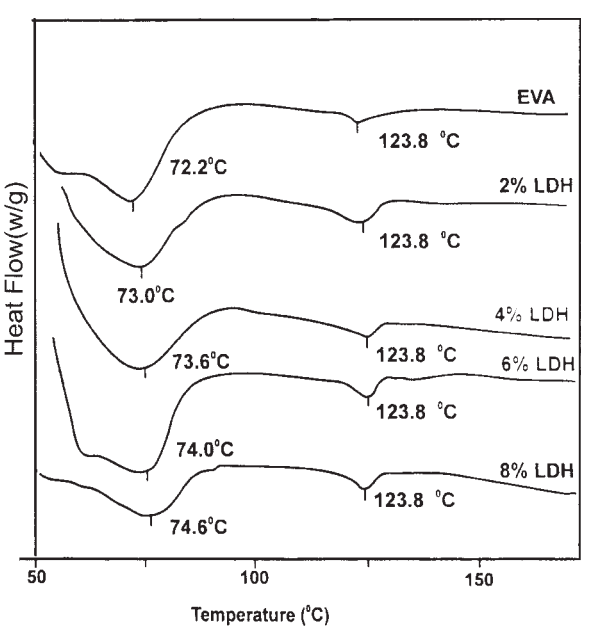

Figure 1 Differential scanning calorimetry traces of EVA/LDH nanocomposite films.

TABLE I
Effect of LDH Nanoparticle Addition on Thermal Properties of EVA Films

Composition weight (%)		Melting temperature (T_m) (°C)	Heat of fusion (ΔH) (J/g)	LOI	UL94
PVA	LDH				
100	00	72.2, 123.8	5.6	19	No rating
98	02	73.0, 123.8	5.1	20	HB
96	04	73.6, 123.8	4.8	21	HB
94	06	74.0, 123.8	4.5	23	V-1
92	08	74.6, 123.8	4.4	26	V-1

spectra of neat EVA and its LDH nanocomposite films were recorded over the wave number range of 500–4000 cm^{-1} using a NICOLET 5700 FT-IR (Thermo Electron Corp.) spectrometer. The tensile properties of solution-casted nanocomposite films (2 mm thickness) were investigated as per ASTM D 882 in universal testing machine (Lloyds UK, Model LR 100K) with a cross head speed of 100 mm/min. Electrical parameter, the arc resistance, was measured as per ASTM D 495 using arc resistance tester (Model: ARC, Sl. No: 101, 2006) supplied by CIPET, Ahmedabad, India and the dielectric strength was measured as per ASTM D 149 using High Voltage Break Down Tester (Model: D/E, Sl. No: 102, 2006) supplied by CIPET, Ahmedabad, India. Moisture content was measured for equilibrated samples in laboratory conditions. Density of the modified films was measured using Mettler PM200 electronic weighing balance as per ASTM D 792 method. The solubility tests were carried out on dried film samples at 23°C ± 2°C and 50% ± 5% RH.

RESULTS AND DISCUSSION

Thermal analysis by differential scanning calorimetry

Differential scanning calorimetry (DSC) is a unique technique to determine the thermal transitions and enthalpies to study the polymer matrix-filler interaction behavior. The DSC thermograms of ethylene vinyl acetate (EVA) copolymer and LDH nanocomposite films with 0, 2, 4, 6, and 8 wt % of LDH nanoparticles are shown in Figure 1. In the neat EVA matrix two melting endothermic peaks are observed at 72.2°C and at 123.8°C corresponding to the melting of VA and methylene blocks (Linear low density polyethylene, LLDPE), respectively. The addition of LDH platelets in the EVA matrix alters melting temperature at 72.2 to 74.6°C. But the melting peak at 123.8°C shows no change. These results indicate that the addition of LDH enters into the VA zone, but not into the crystalline methylene blocks. The increase in melting temperature of VA zone indicates the interaction between VA groups and LDH sheets. These interactions are through the hydrogen bonding between the hydroxyl groups of LDH and acetate groups of EVA.

Table I shows the variation of melting enthalpy as a function of the composition as measured by DSC. Apparently the value of melting enthalpy of VA decreased gradually with increase in LDH content from 5.6 to 4.4 J/g. The decrease in melting enthalpy indicates decrease in crystallinity. The study of the degree of crystallinity is very significant to understand the changes in the structural characteristics induced by LDH. To check whether the filler is located in the crystalline zones of the composite material, this study reports the dependence of the melting enthalpy and the degree of crystallinity on the filler content. It has been reported that the presence of clay also results in modification of crystalline structure of polyamide-6.[34] The presence of clay platelets weakens hydrogen bonding in the polyamide-6[35] or forces the hydrogen bonds out of the plane of the macromolecular sheets.[36] On the other hand, crystal growth is believed to slow down due to mobility

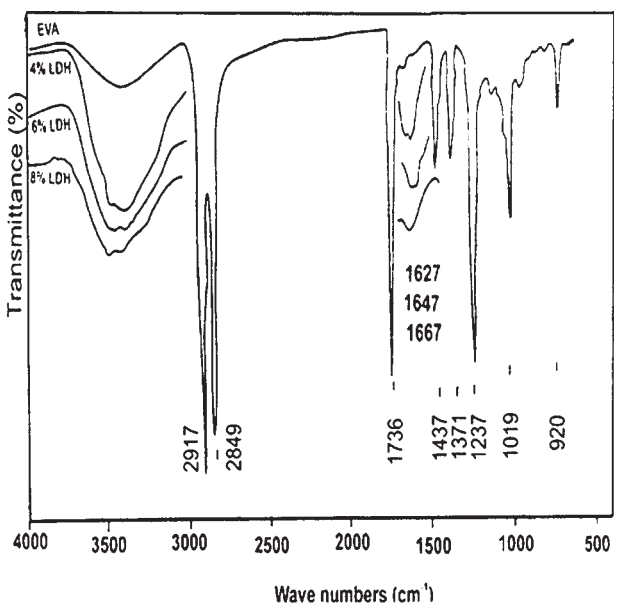

Figure 2 FTIR spectrum of EVA/LDH nanocomposite films.

TABLE II
Band Assignments of FTIR spectra of EVA/LDH Nanocomposite Films

Wave number range (cm^{-1}) for samples					
EVA	2% LDH	4% LDH	6 % LDH	8% LDH	Bands
3,000–3,737	3,035–3,077	2,983–3,741	3,017–3,729	3,000–3,741	O—H band stretch hydrogen bonding
2,917	2,917	2,917	2,917	2,917	Asymmetric vibration of aliphatic $(-CH_2-)_n$ groups
2,849	2,849	2,849	2,849	2,849	Symmetric vibration of aliphatic $(-CH_2-)_n$ groups
1,736	1,736	1,736	1,736	1,736	O—C=O carbonyl stretching vibrations of the esters
–	–	1,627	1,647	1,667	O—H deformation of entrapped water molecules
1,464	1,464	1,464	1,464	1,464	$(-CH_2-)_n$ deformation
1,371	1,371	1,371	1,371	1,371	$(-CH_2-)_n$ wagging
1,237	1,237	1,238	1,238	1,237	Asymmetric vibration of C—O—C bond
1,019	1,019	1,019	1,019	1,019	M—O in plane stretching
720	719	719	719	719	M—O deformation

restriction of the macromolecular chains in the vicinity of the clay.[37,38]

Flammability properties

The LOI estimation and flammability rating of EVA/LDH nanocomposite films are given in Table I. Table I show that the oxygen concentration required to catch fire increased from 19 to 26% and flammability rating enhanced from no rating to V-1 rating with increase in LDH concentration. The flame-retardant characteristics of LDH layers originate from their $Mg(OH)_2$ (MH) like chemistry, which involves endothermic decompositions with the formation of water vapor and metal oxide residue. The residue impedes the burning process by reducing the oxygen supply to the bulk phase under the burning surface. The results shown in the Table I indeed indicate significant improvement in the flame retardancy as characterized by LOI and UL-94 tests.

Fourier transform infrared spectroscopy analysis

The FTIR spectra of neat EVA and its nanocomposite films with 2, 4, 6, and 8 wt % of LDH are shown in Figure 2 and band assignments are shown in Table II. The spectrum has a wide and intense peak from 3000 to 3741 cm^{-1} which is attributed to the O—H band stretch (hydrogen bonding) of the LDH crystal structure. The peaks at 2917 and 2849 cm^{-1} ascribed to the asymmetric and symmetric vibrations, respectively, of aliphatic groups $(-CH_2-)_n$. The position of the carbonyl stretching vibrations does not shift noticeably with increase of LDH content. The band appeared at 1627, 1647, and 1667 cm^{-1} is ascribed to the O—H deformation of entrapped water molecules. The band at around 1464 and 1371 cm^{-1} is attributed to the $(-CH_2-)_n$ deformation and wagging. The band at around 1237 cm^{-1} (1237, 1237, 1238, 1238, and 1237 cm^{-1}) is attributed to the asymmetric vibration of C—O—C bond. The bands at around 1019 and 720 cm^{-1} are ascribed to the metal-oxygen (M—O) in plane stretching and deformation. The FTIR spectral analysis of EVA and its nanocomposite films shows that the addition of LDH into the EVA matrix enhances the width and intensity of the peak at 3000–3741 cm and introduces a new peak (1627, 1647, and 1667 cm^{-1}) corresponding the O—H stretching mode of LDH.

Tensile properties of EVA/LDH nanocomposites

The effect of LDH addition on tensile strength and tensile load at break of EVA matrix is shown in Table III. The tensile strength at break for virgin EVA increased from 2.73 to 5.89 N/mm^2 with increase in LDH loading from 0 to 8 wt %, whereas the introduction of LDH reduces the tensile load at break initially, but subsequent additions enhanced the tensile load from 22.74 to 32.20 N. The stress–strain curves of EVA/LDH (Fig. 3) nanocomposite films show similar trends. The increase in tensile strength with increase in LDH content may be because of the high aspect ratio of nanoparticles that impart excellent reinforcement. These analyses indicate the significance of understanding the interplay between the polymer

TABLE III
Effect of LDH Nanoparticle Addition on Tensile Properties of EVA Films

	Weight percentage of LDH nanoparticles in EVA films				
Tensile property	0	2	4	6	8
Load at beak (N)	40.25	22.74	24.39	24.85	32.20
Tensile strength at break (N/mm^2)	2.73	2.65	2.95	3.47	5.89

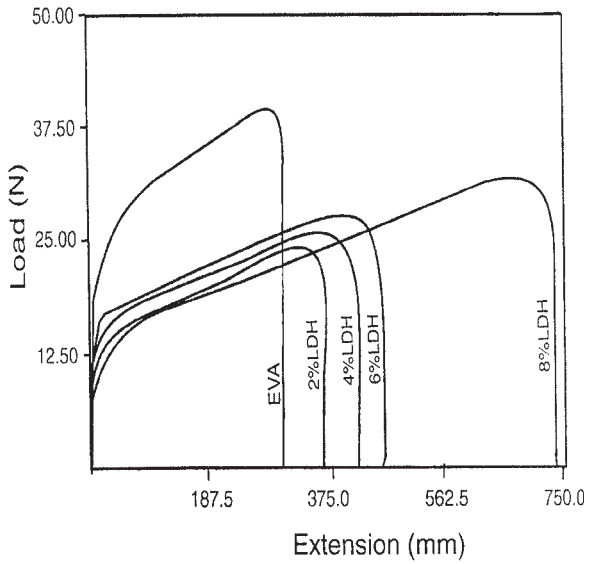

Figure 3 Stress–strain curves of EVA/LDH nanocomposite films.

matrix and LDH concentration in determining the nanocomposite's mechanical properties.

Electrical properties—Arc resistance and dielectric strength

Measurement of arc resistance and dielectric strength for EVA/LDH films in different LDH loadings were carried out to assess the changes in insulation resistance. The results shown in the Table IV indicate that the addition of LDH does not alter the arc resistance and dielectric strength significantly. The dielectric strength of an insulator is defined as the maximum voltage required producing a dielectric breakdown. Arc resistance is the ability of a material to resist the action of a high voltage electric arc, usually stated in terms of time required to form material electrically conductive. Failure is characterized by carbonization of the surface by tracking, localized heating, or burns. Even though the LDH is hydrophilic in nature, the addition of LDH does not alter either the arc resistance (190–197 s) or the dielectric strength (7.6 kV).

Moisture content and density

The moisture content of EVA and its LDH nanocomposite films are shown in Table IV, from the table, it is clear that the filler loading increases the moisture content from 0.28 to 0.79%. The increase in moisture content may be due to the hydrophilic nature of LDH sheets.

The density of EVA/LDH nanocomposite films show gradual increase (Table IV) with increase in LDH loading. The density increased from 0.951 to 0.982 g/cm^3 with increase in LDH content from 0 to 8 wt %. The increase in density may be due to the higher density of LDH filler as well as due to the strong interaction between the LDH and VA groups of EVA.

Solubility resistance

The EVA/LDH nanocomposite films were tested for its resistance in water, DMSO, DMF, glycerol, and xylene (Table V). Since xylene is the solvent for EVA, neat EVA film was dissolved rapidly at room temperature and formed a transparent colorless colloid. The solubility of EVA polymer decreased with increase in LDH content, which may be due to a strong interaction with polymer chains nanolevel-dispersed LDH layers. Indeed, this strong interfacial interaction between the polymer chains and LDH layers inhibits the penetration of xylene molecules from the surface to the bulk region of the nanocomposites, leading to reduction in solubility. Dissolution time of these films increased from 60 to 500 min with increase in LDH content. This enhancement of solubility resistance may be due to the strong interaction and formation of complex structure between EVA and LDH. Further the EVA/LDH films remain virtually unaffected in water, DMSO, DMF, and glycerol. The knowledge of solubility characteristics of a polymer and its nanocomposites is an important aspect for predicting the extent of suitability for their applications in a particular environment. EVA is a highly polar polymer. The acetate groups in EVA contribute to hydrogen bonding with LDH nanoparticles.

TABLE IV
Effect of LDH Nanoparticle Addition on Moisture, Density, Arc, and Dielectric Strength of EVA Films

Composition weight (%)		Moisture	Density	Arc resistance	Dielectric
EVA	LDH	(%)	(g/cm^3)	(s)	strength (kV)
100	00	0.28	0.951	192	7.6
98	02	0.32	0.958	190	7.6
96	04	0.49	0.966	195	7.6
94	06	0.62	0.974	195	7.6
92	08	0.79	0.982	197	7.6

TABLE V
Effect of LDH Nanoparticle Addition on Solubility Characteristics of EVA Films

Composition weight (%)		Dissolution time (min)				
EVA	LDH	Xylene	Water	DMSO	DMF	Glycerol
100	00	60	No change	No change	No change	No change
98	02	90	No change	No change	No change	No change
96	04	125	No change	No change	No change	No change
94	06	330	No change	No change	No change	No change
92	08	500	No change	No change	No change	No change

DMSO, dimethyl sulphoxide; DMF, dimethyl formamide.

CONCLUSIONS

Ethylene-vinyl acetate copolymer (EVA) and Mg-Al LDH nancomposite films have been synthesized with various LDH concentrations by solution (solvent) intercalation process. The melting behavior as well as heat of fusion of the EVA/LDH nancomposite films were studied with DSC and found that the introduction of LDH platelets has increased the melting temperature (T_m) from 72.2 to 74.6°C and reduced heat of fusion (ΔH) from 5.6 to 4.4 J/g. These nanoscale process, driven by the physical and chemical nature of the LDH platelets, enhances the final macroscopic properties of the nanocomposites, such as mechanical properties and flammability. The tensile strength of the nanocomposites increased from 2.73 to 5.89 N/mm^2 and flammability (LOI) rating increased from 19 to 26 with increase in LDH platelets concentration.

References

1. Shin, Y.; Fumio, A. Jpn Pat. 07,041,611 (1995).
2. Hideji, N.; Hideo, S.; Akira, A.; Izumi, I.; Yoji, S. Jpn Pat. 05,170,978 (1993).
3. Mohai, M.; Toth, A.; Hornshy, P. R.; Cusack, P. A.; Cross, M.; Marosi, G. Surf Interface Anal 2002, 34, 735.
4. Marosi, G.; Anna, P.; Bertlam, G.; Szabo, S.; Ravadits, I.; Prap, J; In: Fire and Polymers, Materials and Solutions for Hazard Prevention: Role of Interface Modification in Flame Retarded Multiphase Polyolefin Systems; Nelson, G. L., Ed.; Wilkie: Washington, DC, 2001; p 161.
5. Marosi, G.; Anna, P.; Marton, A.; Bertlam, G.; Bota, A.; Toth, A.; Mohai, M.; Racz, I. Polym Adv Technol 2002, 13, 1103.
6. Marosi, G.; Marton, A.; Anna, P.; Bertlam, G.; Marosfoi, B.; Szep, A. Polym Degrad Stab 2002, 77, 259.
7. Marosi, G.; Marton, A.; Szep, A.; Csontos, I.; Keszei, S.; Zimonyi, F.; Toth, A.; Almeras, X.; Le Bras, M. Polym Degrad Stab 2003, 82, 379.
8. Alexandre, M.; Dubois, P. Mater Sci Eng R 2000, 28, 1.
9. Beyer, G. Plast Addit Compound 2002, 4, 22.
10. Leroux, F.; Besse, J. P. Chem Mater 2001, 13, 3507.
11. Ray, S.; Okamoto, M. Prog Polym Sci 2003, 28, 1539.
12. Ebdon, J. R.; Hunt, B.; Joseph, P.J. Polym Degrad Stab 2004, 83, 181.
13. Vaia, R. A.; Vasudevan, S.; Krawiec, W.; Scanlon, L. G.; Giannelis, E. P. J Polym Sci Part B: Polym Phys 1997, 35, 59.
14. Carrado, K. A.; Thiyagarajan, P.; Elder, D. L. Clays Clay Miner 1996, 44, 506.
15. Strawhecker, K. E.; Manias, E. Chem Mater 2000, 12, 2943.
16. Szep, A.; Szabo, A.; Toth, N.; Anna, P.; Marosi, G. Polym Degrad Stab 2006, 91, 593.
17. Peeterbroeck, S.; Alexandre, M.; Jerome, R.; Dubois, P. H. Polym Degrad Stab 2005, 90, 288.
18. Zhang, X.; Guo, F.; Chen, J.; Wang, G.; Liu, H. Polym Degrad Stab 2005, 87, 411.
19. Chaudhary, D. S.; Prasad, R.; Gupta, R. K.; Bhattacharya, S. N. Thermochim Acta 2005, 433, 187.
20. Chen, W.; Feng, L.; Qu, Q. Chem Mater 2004, 16, 368.
21. Husich, H. B.; Chen, C. Y. Polymer 2000, 44, 5275.
22. Li, B.; Hu, A.; Liu, J.; Chen, Z.; Fan, W. Colloid Polym Sci 2003, 281, 998.
23. Costa, F. R.; Wagenknecht, U.; Jehnichen, D.; Goad, M. A.; Heinrich, G. Polymer 2006, 47, 1649.
24. Alexandre, M.; Beyer, G.; Henrist, C.; Cloots, R.; Rulmont, A.; Jerome, R.; Dubois, P. Macromol Rapid Commun 2001, 22, 643.
25. Alexandre, M.; Beyer, G.; Henrist, C.; Cloots, R.; Rulmont, A.; et al. Chem Mater 2001, 13, 3830.
26. Zanetti, M.; Camino, G.; Thomann, R.; Mulhaupt, R. Polymer 2001, 42, 4501.
27. Zanetti, M.; Kashiwagi, T.; Falqui, F.; Caminom, G. Chem Mater 2002, 14, 881.
28. Duquesne, S.; Jama, C.; Le Bras, M.; Delobel, R.; Recourt, P.; Gloaguen, J. M. Compos Sci Technol 2003, 63, 1141.
29. Ramaraj, B. J Appl Polym Sci 2006, 101, 3062.
30. Ramaraj, B. J Appl Polym Sci 2007, 103, 1127.
31. Ramaraj, B. J Appl Polym Sci 2007, 103, 909.
32. Costa, F. R.; Abdel-Goad, M.; Wagenknecht, U.; Heinrich, G. Polymer 2005, 46, 4447.
33. Costantino, U.; Marmottini, F.; Rocchetti, M.; Vivani, R. Eur J Inorg Chem 1998, 1998, 1447.
34. Kojima, A.; Usuki, A.; Kawasumi, M.; Okada, A.; Kurauchi, T.; Kanigaito, O.; Kaji, K. J Polym Sci Part B: Polym Phys 1994, 32, 625.
35. Wu, Q.; Liu, A.; Berglund, L. A. Polymer 2002, 43, 2445.
36. Lincoln, D. M.; Vaia, R. A.; Wang, Z.-G.; Hsiao, B. S. Polymer 2001, 42, 1621.
37. Fornes, T. D.; Paul, D. R. Polymer 2003, 44, 3945.
38. Mathias, L. J.; Davis, R. D.; Jarret, W. L. Macromolecules 1999, 32, 7958.